Laser-heated miniature pedestal growth apparatus for single-crystal optical fibers

M. M. Fejer, J. L. Nightingale, G. A. Magel, and R. L. Byer

Applied Physics Department, Edward L. Ginzton Laboratory of Physics, Stanford University, Stanford, California 94305

(Received 21 December 1983; accepted for publication 20 July 1984)

We have designed and built a single-crystal fiber growth apparatus. The apparatus employs novel optical, mechanical, and electronic control systems that enable the growth of high optical quality single-crystal fibers. We have grown oriented single-crystal fibers of four refractory oxide materials, Al_2O_3, $Cr:Al_2O_3$, Nd:YAG, and $LiNbO_3$. These materials exhibit similar growth characteristics and yield fibers of comparable quality. Fibers as small as 20 μm in diameter and as long as 20 cm have been grown. Measured optical losses at 1.06 μm for a 10-cm-long, 170-μm-diam $Cr:Al_2O_3$ fiber were 0.074 dB/cm.

INTRODUCTION

The unique combination of material properties and geometry found in single-crystal optical fibers offers intriguing capabilities in a variety of optical devices. Three refractory oxide materials typify the broad range of potential applications.

The large nonlinear coefficients of $LiNbO_3$ suggest its use for modulators, signal processors, and parametric sources. Miniature lasers made from Nd:YAG fibers[1] have been known for several years. Such active fibers might also be used as in-line amplifiers in conventional glass fiber systems. Sapphire's high melting point and favorable optical properties make it useful in applications such as high-temperature thermometry.[2]

The optimal growth or preparation technique to achieve fiber devices in a variety of single-crystal materials is not yet clear. The methods thus far proposed fall into four categories: hot rolling,[3] edge defined growth and its variants,[4–6] Bridgman growth in capillary tubing,[7,8] and miniature pedestal growth.[9,10] The first three growth approaches require a crucible or die with materials that are compatible with the crystal growth conditions. In addition, the small diameter capillaries or orifices necessary to define crystal growth boundaries have to be produced with the same diameter tolerances that apply to the finished fiber. In order to avoid these problems we have chosen to pursue the laser heated pedestal growth method[10] first applied to optical fiber growth by Burrus and Stone.[11]

Our prior efforts to produce optical fiber devices using the pedestal growth method have been hampered by poor fiber quality.[12] In particular, diameter fluctuations and resultant surface irregularities have led to unacceptably large optical transmission losses. We believe these diameter fluctuations stem from mechanical and optical irregularities occurring during fiber growth rather than from some fundamental crystal growth instability. We have thus designed and built a crystal growth apparatus to produce optical quality single-crystal fibers. The present paper focuses on the fiber growth apparatus and reports our initial growth results.

I. REQUIRED FIBER CHARACTERISTICS

The growth of single-crystal fibers is motivated by their application to passive, active, and nonlinear optical devices. The device application determines the required crystal fiber characteristics. Important crystal fiber parameters include length, diameter, and optical attenuation.

Optical loss can stem from a number of causes including bulk crystal imperfections, index of refraction variations, diameter fluctuations, and surface defects. The first two causes of loss are present in conventional crystal growth while the latter two are unique to the fiber geometry. The optical loss induced by surface defects and diameter fluctuations depends strongly on the azimuthal dependence and spatial frequency of the perturbation. We estimate losses on the order of 25% for a 1% random diameter fluctuation in a 5-cm-long, 25-μm-diam fiber.

The optical losses can be reduced by using a diffused cladding if the diffusion depth is large compared to the scale length of the diameter variations. Diffused cladding could be accomplished in different ways; for example, out diffusion of Cr^{+3} ions from ruby fibers[13] or in diffusion of protons in *c*-axis $LiNbO_3$ fibers.[14]

Most optical crystal fiber devices require fiber lengths less than 5 cm with fiber diameters below 200 μm. Small fiber diameters are particularly important in nonlinear optical devices, since tight beam confinement leads to improved nonlinear conversion efficiency. In some passive device applications, such as high-temperature sapphire thermometry,[2] the acceptable optical losses can be quite large and thus fiber diameter variations of several percent are tolerable. Nonlinear interactions, particularly those involving a fiber within a resonator, are more sensitive to diameter fluctuations. We estimate that for a nondiffused cladding, diameter fluctuations must be in the 0.1%–1% range for a useful nonlinear fiber. We have designed and built a crystal growth

 0034-6748/84/111791-06$01.30

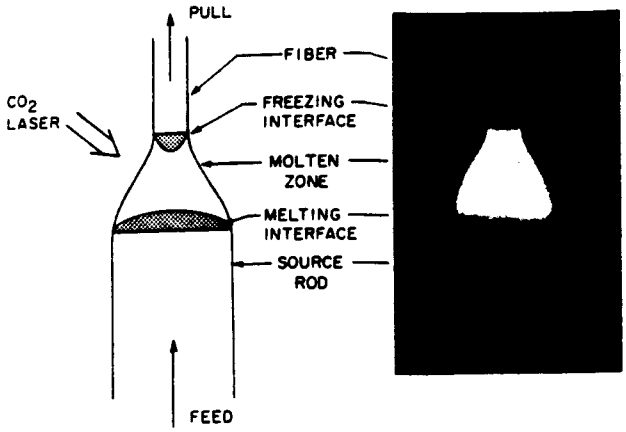

FIG. 1. Schematic diagram and corresponding photomicrograph of fiber growth. The photomicrograph depicts growth of a 190-μm $LiNbO_3$ fiber from a 570-μm-diam source rod. The fiber is supported from above by wetting an oriented seed crystal (not shown). The growth ridges faintly visible on the fiber are discussed later in the text.

apparatus to grow fibers with these length, diameter, and diameter stability characteristics.

II. DESCRIPTION OF GROWTH APPARATUS

A. Design overview

Figure 1 illustrates the miniature pedestal growth of a single-crystal fiber. A tightly focused CO_2 laser, emitting 10.6-μm radiation is the heat source used to melt the refractory material. The source rod may be fabricated from single-crystal,[11] polycrystalline, sintered,[13] or pressed power[15] material. The seed rod defines the crystallographic orientation of the fiber. Growth proceeds by simultaneous upward translation of the seed and source rods with a molten zone positioned between them. The laser focal spot, and consequently the molten zone, remain fixed during fiber growth. The source rod to fiber diameter ratio is set by mass conservation to be the square root of the fiber to source rod translation rate. Typical fiber growth rates range from 1–10 mm/min with diameter reductions of approximately three.

In our system ground rods 500 μm in diameter serve as the initial source for fiber crystal growth. The small rod diameter provides the ability to grow materials with melting points exceeding 2000°C using only a few watts of laser power. An initial growth step reduces the 500-μm-diam rods to a 170-μm-diam fiber. Subsequent diameter reductions using the fiber as a source rod are also possible.

In order to achieve a constant fiber diameter, stable fiber growth conditions must be realized. This in turn dictates smooth source feed and fiber pull rates, stable laser power, and symmetric heat input into the molten zone.

B. Optical system

A block diagram and photograph of the fiber growth apparatus are shown in Figs. 2 and 3, respectively. A 15-W polarized waveguide CO_2 laser (California Laser, model 82-15000-P-W)[16] served as the heat source for crystal growth. The water-cooled laser cavity is temperature stabilized and produces a polarized HE_{11} output mode with power fluctuations less than 1%.

The laser power and beam pointing are most stable if the laser is allowed to run at constant high power. Therefore, an electro-optic power control system is used to vary the laser power incident on the molten zone. The system consists of a ZnSe quarter-wave plate, CdTe electro-optic crystal, and ZnSe polarizer/analyzer. The measured system dynamic range is greater than 100:1. Provisions for modulating the incident laser power have been incorporated into the control circuitry to allow growth of a fiber with controlled diameter variations. Such periodic variations could serve as a distributed Bragg reflector eliminating the need for conventional mirrors in fiber resonator devices.

The CO_2 laser beam (invisible) emerging from the polarizer is combined with a HeNe laser beam (visible) on a dichroic mirror. The visible coincident HeNe beam facilitates CO_2 alignment down the remainder of the optical train. After passing through a ZnSe focusing telescope and some beam steering optics, the CO_2 beam enters the controlled atmosphere growth chamber.

Within the growth chamber a novel optical system focuses the laser beam onto the fiber in a 360° axially symmet-

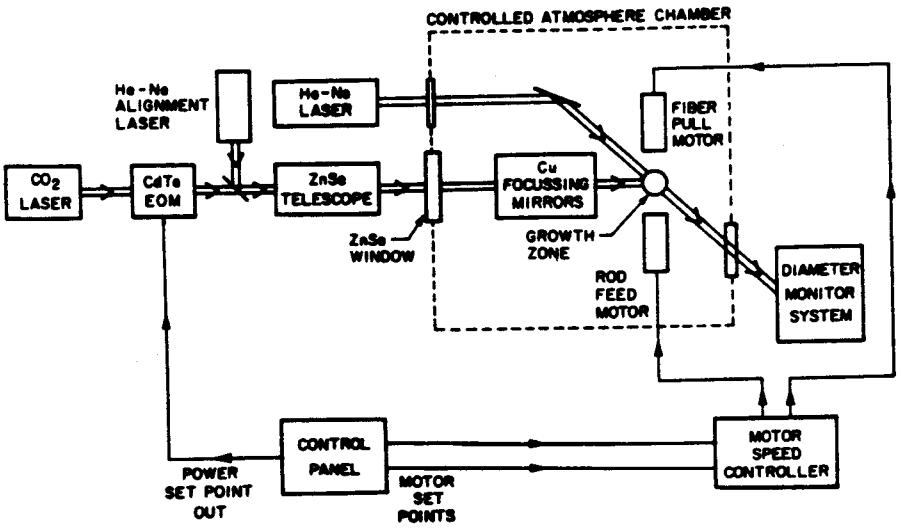

FIG. 2. Block diagram of fiber growth apparatus.

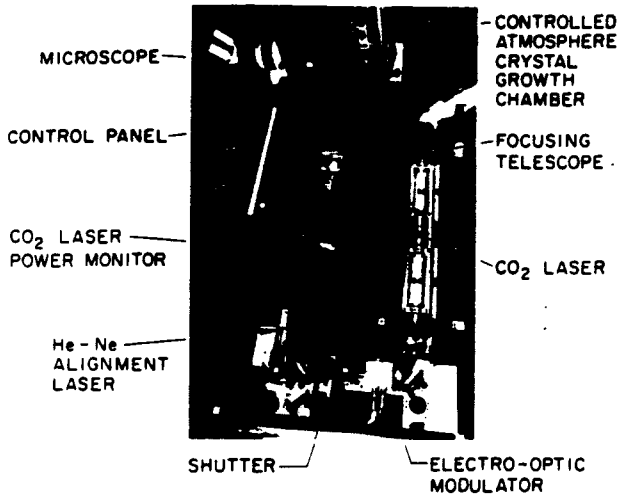

FIG. 3. Photograph of fiber growth apparatus. The diameter measurement system is not installed. A plastic dust cover which normally protects the optical train has been removed for the photograph.

ric distribution as shown in Fig. 4. The symmetric irradiance prevents cold spots in the growth zone and represents a significant improvement over the previously used two-beam,[13] rotating periscope,[17] or ellipsoidal[18] focusing systems. An optical element incorporated into the design is a reflaxicon,[19] which consists of an inner cone surrounded by a larger coaxial cone. In order to achieve good optical performance it is critical that the reflaxicon's two cones be accurately aligned.

A mated surface design, using diamond turned copper optical components, manufactured by Pneumo Precision,[20] assures centering of the two cone axes. A gold coating on the copper optical surfaces enhances reflectivity and protects the copper substrate. The reflaxicon and parabolic mirror provide near diffraction limited $f/2$ focusing, yielding a minimum spot size of 30 μm. This tight focus is important for the stable growth of small diameter fibers. The focal spot size can be controlled by modifying the input beam divergence with the focusing telescope. Motorized x–y states on the fiber and source rod translation devices permit adjustment of the fiber position with respect to the fixed laser focal spot.

C. Mechanical system

Previous miniature pedestal growth systems have used lead screw translation. The lead screw fiber translation approach has the drawback that the fiber support point moves away from the melt zone as the fiber grows. The growth zone is thus increasingly sensitive to mechanical perturbations for small diameter and/or long fibers. Moreover, lead screw travel limits the total fiber length.

To alleviate these problems we adopted the belt drive system shown in Fig. 5. The fiber is driven by a polyester cord reinforced urethane belt, which in turn is driven by a dc motor through a speed reducing gearhead. An optical encoder, attached to the dc motor, allows locking the motor speed to a stable reference frequency. A V groove etched in silicon[21] and overcoated with SiO_2 guides the fiber to prevent

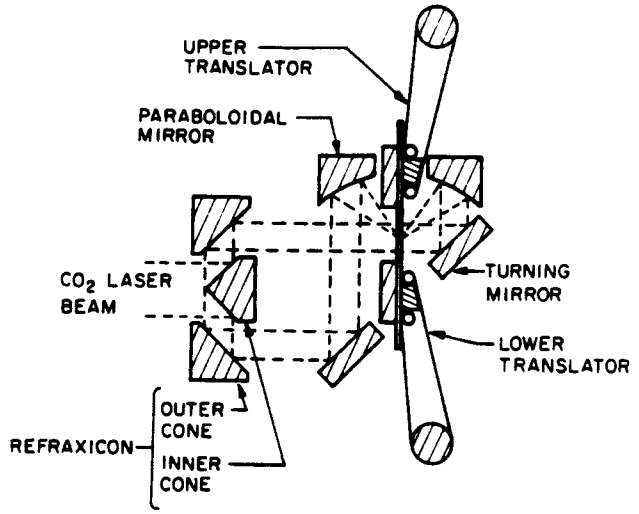

FIG. 4. Photograph of sapphire fiber growth showing optical focusing elements and head of lower translator. A cross-sectional diagram of focusing optics and translators is also shown.

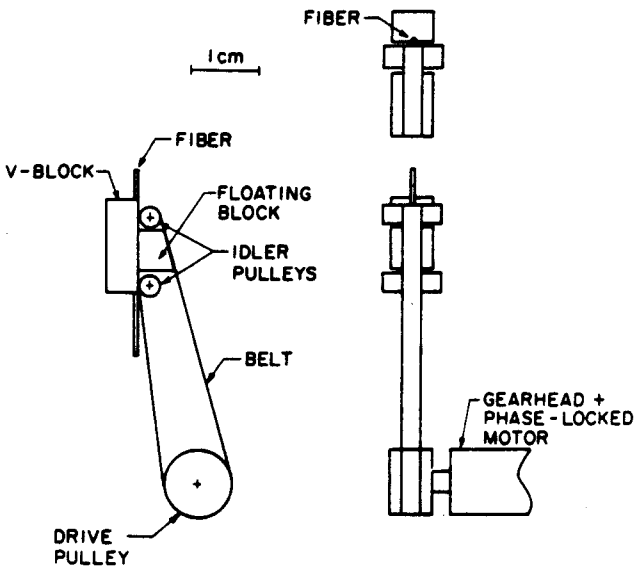

FIG. 5. Detail of fiber translator.

side-to-side wobble. It provides a smooth, hard sliding surface along the fiber axis.

A phase-locked control circuit enables stable dc motor operation over a 100:1 speed range with acquisition times of 100 ms. A useful control option allows fixing the fiber to source rod speed ratio while adjusting growth speed. Since the fiber diameter has starting transients in the initial phases of growth, a slow growth rate allows time for the operator to make adjustments. As equilibrium conditions are reached growth speed can be conveniently increased without changing the fiber diameter.

The motor control system ensures motor velocity stabilization to frequencies above the mechanical response time of the drive system. Gear noise introduced in the speed reducing gearhead between the dc motor and belt drive pulley is a possible source of fiber translation fluctuation. The magnitude of this noise is not known. However, measurements of the actual fiber translation velocity indicate a jitter of less than 3%, the measurement resolution.

Fiber motion orthogonal to the translation direction is limited only by fiber straightness and diameter uniformity. Uniform diameter source rods are fabricated using a Boccadoro[21] model FB40 centerless grinder. We have ground rods of Al_2O_3, YAG, and $LiNbO_3$ to diameters of 300–600 μm in lengths up to 12 cm, with a taper of less than 1 μm/cm. For these source rods, the measured side-to-side wobble during translation is less than 3 μm, the measurement resolution.

During growth the molten zone is situated 1 cm above the lower translator. The upper translator has two operating positions, 1 and 3.5 cm above the melt. The raised position allows growth of an approximately 3-cm-long fiber without the newly grown fiber contacting the translator. The seed for this growth is typically an oriented crystal mounted in a capillary tube.

Longer fiber lengths are obtained using the lower position of the upper translator and a previously grown 3-cm-long fiber as a seed crystal. In this case both the newly grown fiber and the seed crystal pass through the upper translator. The diameter of the fiber must be matched to that of the seed crystal to within $\pm$ 10% to avoid jamming the translator. The small irregularities in fiber diameter resulting from the joint between the seed crystal and new growth can give rise to unacceptably large molten zone side-to-side wobble. This forces the addition of an 8-mm-long glass capillary tube guide mounted onto the end of the upper translator. For growth of a 170-μm-diam fiber a 200-μm-diam guide provides the necessary position stability.

D. Diameter measurement system

Another important feature of the growth apparatus is a high-speed noncontact diameter measurement system. As currently used the system monitors the fiber diameter during growth. A planned improvement in the growth apparatus will be to use the diameter measurement system to provide an error signal in a diameter stabilization feedback loop. In order to grow fibers with 0.1% diameter stability at mm/min growth rates the diameter measurement system must have a measurement rate >100 Hz, a diameter resolution <0.05%, an axial resolution as small as 5 μm, and a working distance >100 mm to avoid obstruction of the CO_2 focusing system. No commercial system was available which met all these criteria.

We designed and built the fiber diameter system shown schematically in Fig. 6. A helium–neon laser beam illuminates one side of the fiber. The rays passing through the fiber and those reflected off the fiber surface interfere in the far field to form a series of light and dark fringes whose period is inversely proportional to the fiber diameter.[23] By imaging the interference pattern on a photodiode array and electronically tracking one of the fringes as it changes position in response to fiber diameter changes, a voltage proportional to the diameter change is derived. As built, the system has a diameter resolution better than 0.02%, an axial resolution of 5 μm, and a measurement rate of 1 kHz. A detailed description of the diameter measurement system is given by Fejer, Magel, and Byer.[24]

III. RESULTS

Four crystalline materials have been grown to date: sapphire (Al_2O_3), sapphire with 0.05 wt.% chromium (ruby), YAG with 0.9 wt.% neodymium, and lithium niobate ($LiNbO_3$). Growth characteristics of the chromium doped ruby were identical to those of the pure sapphire. Growth orientations for the fibers were ⟨001⟩ for sapphire, ⟨111⟩ for YAG, and both ⟨001⟩ and ⟨100⟩ for lithium niobate. Fibers as small as 20 μm in diameter and as long as 20 cm have been grown (see Table I). Fiber growth speeds ranged from 0.3 to 30 mm/min.

Typical diameter reductions are approximately three to one. Larger diameter reductions result in less stable growth and yield fibers with larger diameter fluctuations. Smaller diameter reductions yield good quality fibers but require more steps to reach the desired diameter. The observed correlation between diameter reduction and growth stability agrees qualitatively with the theoretical analysis of Surek and Coriell.[25]

Even though the melting temperatures range from 2045° to 1260 °C for these materials, their fiber growth characteristics are similar. Molten zone length is determined by the incident laser power. For optimum growth stability the laser power was adjusted to yield the molten zone shape depicted in Fig. 7. For all materials investigated the optimal molten zone shape is similar, with a height–width ratio of

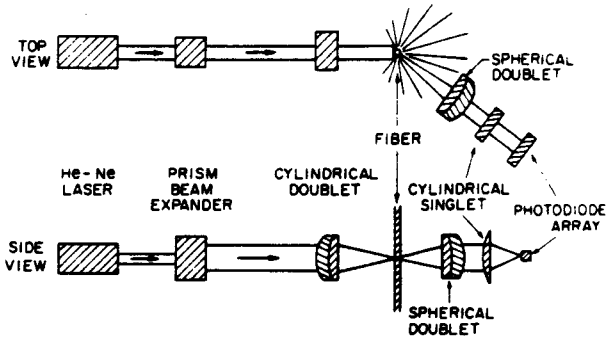

FIG. 6. Schematic diagram of fiber diameter measurement system.

I. Length, diameter, and crystallographic orientation for some single-crystal fibers grown with the apparatus.

Material	Orientation	Length (cm)	Diameter (μm)
Al_2O_3	⟨001⟩	20	170
		3.0	50
Al_2O_3 + 0.05 wt.% Cr	⟨001⟩	10.0	170
		3.0	20
YAG + 0.9 wt.% Nd	⟨111⟩	3.0	110
		3.0	40
$LiNbO_3$	⟨001⟩	3.0	50
	⟨100⟩	3.0	170

0.9 ± 0.15 for a 3 to 1 diameter reduction. Typical power levels necessary to grow from 500-μm Al_2O_3 or $LiNbO_3$ rods are 4.8 and 1.5 W, respectively.

In Fig. 7 the growing fiber is invisible since its smooth sides scatter much less light than those of the ground source rod. The solid–liquid growth interface is evident as the slightly darker bowl-shaped region at the top of the molten zone. The curvature of this isothermal surface reflects the radial temperature gradients present. The measured angle between the growing fiber and the molten zone at the periphery (meniscus angle) is 12° and 8° ($\pm 2°$) for sapphire and YAG, respectively. This angle is a material constant independent of fiber growth speed or diameter. Our measured meniscus angle for sapphire ($12° \pm 2°$) is slightly below but not inconsistent with the $17° \pm 4°$ value previously measured by Dreeben, Kim, and Schujko.[28]

A well-defined meniscus angle could not be measured in lithium niobate due to the highly anisotropic fiber cross section. *A*-axis lithium niobate fibers shows a rectangular cross section with two protruding ridges, while *c*-axis lithium niobate has three sharply defined growth ridges. These ridges are clearly shown in Figs. 8(a) and 8(b). The ridges run smoothly and continuously down the length of the fiber as shown in Fig. 8(c). The growth ridges found in $LiNbO_3$ are not evident in either sapphire or YAG fibers, both of which show a slightly rounded hexagonal cross section.

Another feature evident in Fig. 8(c) is the excellent fiber diameter control and surface quality. No fiber irregularities exist on the micron scale lengths visible in the figure. On a longer scale length we have demonstrated a rms diameter variation of 1% over a 1 cm length of fiber.

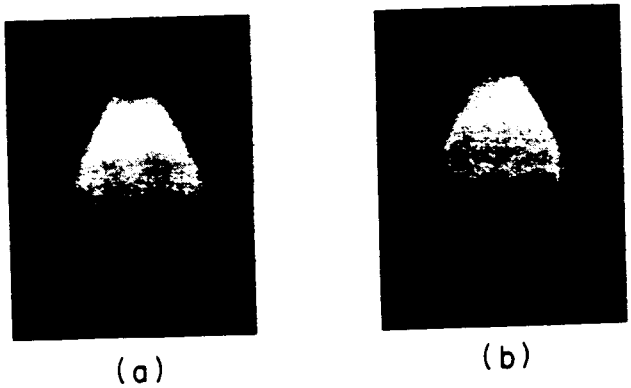

FIG. 7. Both photomicrographs illustrate a 3 to 1 diameter reduction from a 500-μm-diam source rod. Materials are (a) Al_2O_3, melting point 2045 °C and (b) Nd:YAG, melting point 1970 °C. Notice the similarity to Fig. 1 showing $LiNbO_3$, melting point 1260 °C.

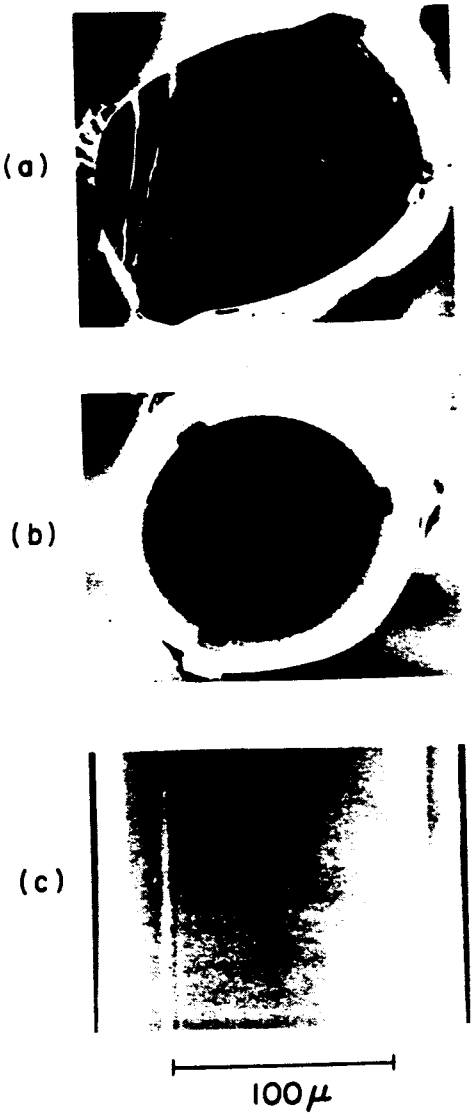

FIG. 8. Scanning electron micrographs of $LiNbO_3$ fibers: (a) cleaved cross section of *a*-axis fiber, (b) cross section of *c*-axis fiber, (c) surface of *c*-axis fiber. The internal concentric ring pattern and dark central area in (b) are artifacts of the procedure used to obtain the cross section. In (c) note the sharply defined growth ridges at the right boundary and near the left edge.

Typical variations in fiber diameter are shown in Fig. 9. This 55-μm-diam ruby fiber was grown at 4.5 mm/min from a 165-μm-diam source rod. The previously described diameter measurement apparatus was used to measure the deviations about the mean diameter. The rms diameter variation over the entire fiber length is 1.7%. The last centimeter of fiber shows a 1% rms diameter variation.

To date all growth has been performed with the growth chamber open to the atmosphere. The as-grown $LiNbO_3$ fibers have a brownish cast resulting from oxygen loss during growth. Annealing the fiber at 1000 °C in an oxygen atmosphere for several hours recovers a water-white crystal color.

A 10-cm-long, 170-μm-diam ruby fiber grown at 3.0 mm/min showed 72% transmission of an incident 1.06-μm

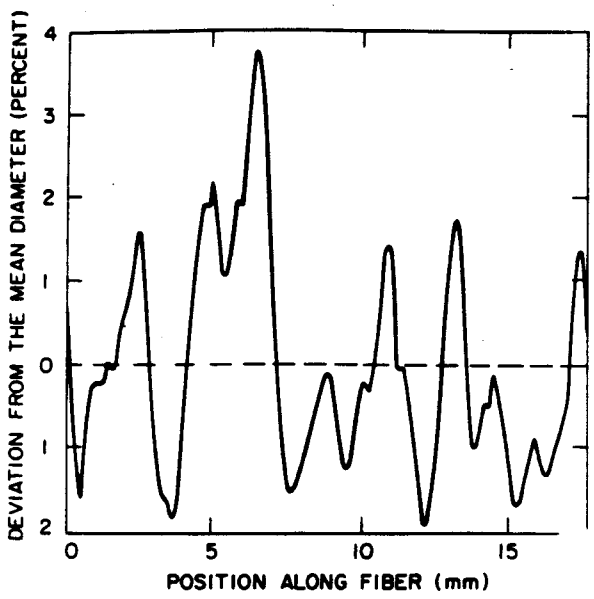

FIG. 9. Diameter variations in a 55-μm-diam ruby fiber measured with the noncontact diameter measurement system.

Nd:YAG laser beam. Taking into account the Fresnel reflection losses from the fiber end faces, the fiber optical loss can be calculated as 1.7%/cm or equivalently, 0.074 dB/cm. In this test no optical cladding was used, the guiding dielectric interface being the ruby fiber surface and the surrounding air.

IV. DISCUSSION

The single-crystal fiber growth apparatus has proven very reliable and easy to use. Over the past year six different operators have grown a total of more than 350 fibers. As many as 14 fibers have been grown on a single day. The time necessary to change from growing one material to another is small, approximately 30 min.

The novel design of the apparatus has allowed the growth of single-crystal fibers with a diameter stability of 1% per centimeter of length. The growth morphology of the crystal fibers is similar to that seen in bulk Czochralski crystal growth. The noncircular nature of the fiber cross section does not introduce additional optical loss since the cross section is invariant with length.

In our initial efforts to propagate light down these fibers we have measured optical losses of $<2\%$ per cm over distances of several centimeters. Losses of this level are acceptable in some device applications such as sapphire fiber thermometry. Efficient active and nonlinear devices demand somewhat lower optical losses. We have designed and constructed a single-crystal fiber growth apparatus based on a laser heated miniature pedestal growth technique. Oriented single-crystal fibers have been grown with diameters of 500 to 20 μm. Planned improvements in fiber diameter control and fiber cladding techniques should allow realization of single-crystal fiber-optical devices.

ACKNOWLEDGMENTS

We gratefully acknowledge useful discussions with M. Digonnet, D. L. O'Meara, T. Y. Fan, W. Kozlovsky, G. A. Kotler, R. S. Feigelson, R. K. Route, and W. Kway, all of Stanford University. We are thankful for the technical support provided by D. Buseck, S. Greenstreet, J. J. Vrhel, M. M. Simkin, K. L. Doty, A. Ospina, B. A. Williams, and P. A. Thompson. This work was supported by the Joint Services Electronics Program, Contract No. N00014-75-C-0632, the Air Force Office of Scientific Research, Contract No. 83-0193, The Stanford University Center for Materials Research, Contract No. CMR-80-20248, and the Lawrence National Laboratories at Livermore, Contract No. 8518101. G. A. Magel gratefully acknowledges the support of the Fannie and John Hertz Foundation.

[1] J. Stone and C. A. Burrus, Fiber Integrated Opt. **2**, 19 (1979).
[2] R. R. Dils, J. Appl. Phys. **54**, 1198 (1983).
[3] J. A. Harrington, Proc. SPIE **227**, 85 (1980).
[4] J. T. Bridges, J. S. Hasiak, and A. R. Strand, Opt. Lett. **5**, 85 (1980).
[5] H. E. La Belle, Jr. and A. I. Mlavsky, Mater. Res. Bull. **6**, 571 (1971).
[6] B. Chalmers, H. E. La Belle, Jr., and A. I. Mlavsky, Mater. Res. Bull. **6**, 681 (1971).
[7] J. L. Stevenson and R. B. Dyott, Electron. Lett. **10**, 449 (1974).
[8] H. P. Weber, P. F. Liao, B. C. Tofield, and P. M. Bridenbaugh, Appl. Phys. Lett. **26**, 692 (1975).
[9] D. B. Gasson and B. Codkayne, J. Mater. Sci. **5**, 100 (1970).
[10] J. S. Haggerty, NASA Report No. Cr-120948, 1972.
[11] C. A. Burrus and J. Stone, Appl. Phys. Lett. **26**, 318 (1975).
[12] M. Fejer, R. L. Byer, R. Feigelson, and W. Kway, *Proceedings of the SPIE Advances in Infrared Fibers II* (1982), p. 320.
[13] C. A. Burrus and L. A. Coldren, Appl. Phys. Lett. **31**, 383 (1977).
[14] J. L. Jackel, C. E. Rice, and J. J. Vaselka, Jr., Appl. Phys. Lett. **41**, 607 (1982).
[15] J. Stone and C. A. Burrus, J. Appl. Phys. **49**, 2281 (1978).
[16] California Laser Corporation, 1070 Commerce Street, San Marcos, CA 92069.
[17] J. E. Midwinter, *Optical Fibers for Transmission* (Wiley, New York, 1979), p. 194.
[18] U. C. Paek, Appl. Opt. **13**, 1383 (1974).
[19] W. R. Edmonds, Appl. Opt. **12**, 1940 (1973).
[20] Pneumo Precision Incorporated, Precision Park, Keene, NH 03431.
[21] F. Boccadoro, Via Dr. Varesi, CH-6600 Locarno, Switzerland.
[22] C. M. Schroeder, BSTJ **57**, 91 (1978).
[23] D. H. Smithgall, L. S. Watkins, and R. E. Frazee, Jr., Appl. Opt. **16**, 2395 (1977).
[24] M. M. Fejer, G. A. Magel, and R. L. Byer (to be published).
[25] T. Surek and S. R. Coriell, J. Cryst. Growth **37**, 253 (1977).
[26] W. Bardsley, F. C. Frank, G. W. Green, and D. T. J. Hurle, J. Cryst. Growth **23**, 341 (1974).
[27] T. Surek, J. Appl. Phys. **47**, 4384 (1976).
[28] A. B. Dreeben, K. M. Kim, and A. Schujko, J. Cryst. Growth **50**, 126 (1980).